Reassessment of the basis of cell size control based on analysis of cell-to-cell variability

Giuseppe Facchetti[1,*], Benjamin Knapp[2], Fred Chang[2,*], Martin Howard[1,*]

[1]John Innes Centre, Computational and Systems Biology, Norwich, United Kingdom

[2]University of California San Francisco, Cell and Tissue Biology, San Francisco, CA, USA

* Corresponding authors

Giuseppe Facchetti Giuseppe.Facchetti@jic.ac.uk

Fred Chang Fred.Chang@ucsf.edu

Martin Howard Martin.Howard@jic.ac.uk

ABSTRACT

Fundamental mechanisms governing cell size control and homeostasis are still poorly understood. The relationship between sizes at division and birth in single cells is used as a metric to categorize the basis of size homeostasis [1-3]. Cells dividing at a fixed size regardless of birth size (sizer) are expected to show a division-birth slope of 0, whereas cells dividing after growing for a fixed size increment (adder) have an expected slope of +1 [4]. These two theoretical values are, however, rarely experimentally observed. For example, rod-shaped fission yeast *Schizosaccharomyces pombe* cells, which divide at a fixed surface area [5, 6], exhibit a division-birth slope for cell lengths of 0.25±0.02, significantly different from the expected sizer value of zero. Here we investigate possible reasons for this discrepancy by developing a mathematical model of sizer control including the relevant sources of variation. Our results support *pure* sizer control and show that deviation from zero slope is exaggerated by measurement of an inappropriate geometrical quantity (e.g., length instead of area), combined with cell-to-cell radius variability. The model predicts that mutants with greater errors in size sensing or septum positioning paradoxically appear to behave as better sizers. Furthermore, accounting for cell width variability, we show that pure sizer control can in some circumstances reproduce the apparent adder behaviour observed in *E. coli*. These findings demonstrate that analysis of geometric variation can lead to new insights into cell size control.

SIGNIFICANCE

How cells control their size is a fundamental but still open question. It has been assumed that the two principle methods of control, namely sizer (where cells always divide at a fixed size) and adder (where cells always add a fixed size increment), can be identified because the correlation between size at birth and size at division is equal to 0 and to +1, respectively. However, experiments mainly provide numbers in between these two values. We show that use of cell length as the size measure, together with cell-to-cell radius variability, can explain this discrepancy and support pure sizer control in fission yeast. Surprisingly, the same phenomenon might exclude adder control in bacteria like *E. coli*.

INTRODUCTION

Cell growth and cell division are coordinated during the cell cycle such that the size of a cell is maintained around a target value specific for each organism and cell type. However, how this outcome is achieved is still largely an open question. Investigations of cell size control intrinsically require a quantitative experimental approach, with many investigations focusing on the simple geometries of yeasts and bacteria. In fission yeast, analyses of individual cells show that they grow to a surface area of about 160 μm^2 before entering mitosis and dividing [6]. Phenomenological characterization of size homeostasis, measuring birth and division sizes of individual single cells, has shown that cells grow to a specified size regardless of birth size. These findings suggest that these cells monitor their own size, dividing at the same size regardless of the size at birth [1, 4, 7]. This principle is called sizer control. On the other hand, the same analysis on *E. coli* data reveals that these cells appear to add a constant size increment during each cell cycle [3, 8], so-called adder control. These cells show a positive correlation between size at birth and size at division [4, 9], so that shorter (longer) cells tend to divide shorter (longer). Theoretical studies have further investigated adder control in terms of robustness to stochastic perturbations and their consequences for the duration of different cell cycle phases [10, 11].

The interpretation of these measurements assumes an unambiguous correspondence between the observed behaviour (division-birth size correlation) and the underlying basis of size control. No correlation implies cells with pure sizer control; a perfect correlation implies cells with pure adder control. However, experimental data has revealed correlations that lie in between these two cases, results which have challenged the notion of a simple basis for size control. As a result, controversies over the basis of size control persist even in *E. coli* (sizer versus adder [12]), as well as in budding yeast (sizer versus adder [2, 13]), whereas a recent study has proposed a combination of a timer (fixed time duration cell cycle) and an adder for *C. crescentus* [14]. Because of its stereotypical shape, and greater available understanding, this work considers fission yeast as a reference model. Even in this case, the measured division-birth correlation is significantly different from zero, casting some doubt on the sizer hypothesis [15].

Previous work showed that size homeostasis in fission yeast is based on total surface area sensing (rather than on cell length or volume sensing) [5, 6]. Quantitative measurements support the idea that this surface area control is achieved by accumulation of Cdr2 in protein clusters ("nodes") in a cortical band around the nucleus. As a result of this localization, the Cdr2 local nodal density scales with cell surface area, which can then trigger mitosis via thresholding [5, 6]. Moreover, through use of a *cdr2-T166A rga2*Δ mutant, cell size homeostasis was successfully switched to length-based size control, confirming the key role of Cdr2 protein in the mechanism [6]. Critical to these conclusions were analyses of mutant cells with altered widths, using *rga2*Δ (thinner) and *rga4*Δ (fatter) mutants [6, 16, 17], which allowed for a robust distinction to be made between size controls based on length, area or volume. However, most data from the literature uses length as

the measure of cell size [1, 7, 15] and for wild-type cells shows a significantly positive division-birth slope (approximately from 0.2 to 0.3), suggesting that cells might inherit and preserve some elements of size information from the previous cell cycle, similar to adder behaviour. Our data (Fig. 1A) shows a similarly positive division-birth slope of around 0.25. Clearly, these findings are not straightforwardly consistent with pure sizer control [6].

This non-zero slope raises the possibility that cells may display pure size control that is obscured by measurement errors or other sources of variability (Fig. 1B). Alternatively, cells might adopt an imprecise implementation or some "impure" mixture of adder and sizer controls (Fig. 1C). To test these possibilities, we sought to determine what division-birth correlations would be generated by pure sizer (or adder) control, if the relevant sources of variation were properly accounted for. Our first result is that we can explain all the correlations experimentally observed for fission yeast in terms of pure sizer control only. Experimentally measuring a geometrical measure of cell size (length) that is different to that intrinsically used by the cells in their size control (area), together with radius variability within the cell population, can generate a large shift of the division-birth slope to higher values. We surprisingly found that a reduction in size-sensing precision by the cell, or in the precision of placement of the division plane, can paradoxically appear to generate better sizer behaviour in a division-birth plot. These insights also apply to size control in *E. coli*, indicating that our approach may improve the assessment of cell size homeostasis control in many cell types.

RESULTS

Sources of variation and mathematical model

In order to improve our understanding of the variety of size homeostasis behaviours, we developed a simple mathematical model of pure area-based sizer control in fission yeast, including the relevant sources of variation in cell size regulation and measurement (Materials and Methods). Since a sizer mechanism is based on size sensing only, the model does not contain time as a variable and, therefore, we do not need to include any error in the duration of the cell cycle. We aimed to test whether such a model is sufficient to reproduce the apparently imperfect sizer behaviour observed above. We assumed that each source of variation is Gaussian distributed, with the free parameters being the following standard deviations: σ_μ (error μ that cells make in sensing size and therefore in mitotic commitment), σ_α (error giving asymmetric placement α of the division plane with respect to the exact mid-plane of the cell) and σ_ρ (natural cell-to-cell variability ρ of the radius). We also included σ_ε as the standard deviation of the measurement error ε (μm) due to image acquisition and segmentation (see Table 1 for the entire list of variables and parameters of the model). As an example, the measured cell radius (R^*, where in the following the mark * will denote a measured quantity) is given by $R^* = R(1+\rho)+\varepsilon$, where R is the mean radius of the cell population (see Materials and Methods). Similar expressions can also be derived for the length at birth and length at division. From these equations, we

can calculate the coefficient of variation (CV) for all geometrical quantities at division (Materials and Methods). For instance, in case of the division length, the CV is given by the sum of three contributions:

$$\mathrm{CV}_{L_d^*}^2 \approx \sigma_\mu^2 + \sigma_\rho^2 + \left(\frac{2\pi R}{A}\right)^2 \sigma_\varepsilon^2. \quad (1)$$

Compared to simple probabilistic sizer models for which cells divide according to a probability of division as a function of cell size [2, 18], our equation describes the distribution of sizes at division as a combination of well-defined sources of error.

We first estimated the model parameters. All parameters, except for the noise σ_α due to asymmetry in division, were obtained by fitting to the measured CV of radius, length, area and volume at division (which are all clearly unaffected by σ_α). We utilised images of wild-type cells acquired at different z-planes (to guarantee good focus). We then generated (and re-segmented) images at four different resolutions, i.e. with different values of the experimental error σ_ε. This was achieved by binning a square of *n* by *n* pixels into a single pixel, with *n* ranging from 1 to 4, i.e. four different values of σ_ε (Fig. 2A). Cells were then segmented using an algorithm specific for rod or quasi-rod shaped cells (Materials and Methods). For each of the four geometrical quantities (radius, length, area and volume), and for each resolution, we measured the coefficient of variation of division size. We then fitted these data points with the model equations by tuning the 6 model parameters (σ_μ, σ_ρ and the four values of σ_ε). The minimal Root Mean-Square Deviation (RMSD) was obtained with $\sigma_\mu = 6.5\%$ and $\sigma_\rho = 2.7\%$ (Fig. 2B and S1). Finally, through measurement of the localization of the septum, we directly estimated the asymmetry in division in wild-type cells (Materials and Methods). By knowing σ_ε , we obtained the value of $\sigma_\alpha = 3.2\%$, consistent with literature reports [19] (Fig. 2C).

From the above estimation, we note the value of 6.5% for the area sensing error, which is smaller than the CV of the division length (about 7-8%) normally used to indicate the accuracy of size sensing [7]. This initial result indicates that the sizer mechanism in fission yeast is slightly more precise than previously thought.

Alteration of cell radius variability supports pure sizer control

Most of the analysis reported in the literature on rod-shaped cells is based on length, because length is the easiest quantity to measure. Therefore, it is important to find an appropriate way to interpret the outcomes from these measurements. In this case, our data for the wild-type alone shows a positive birth-division slope: 0.25±0.02 (Fig. 1A, S2, consistent with available values [1, 7, 15]). We next investigated whether these discrepancies were due to errors, and whether this data could support the existence of pure sizer control in fission yeast.

From the expressions of the measured length at birth (L_b^*) and measured length at division (L_d^*), while still having underlying area-based size control, we can derive an equation for the theoretical value of the division-birth slope (Materials and Methods):

$$\mathrm{slope}(L_d^*, L_b^*) = \frac{2\sigma_\rho^2}{H^2\sigma_\rho^2 + K^2}, \tag{2}$$

where $H^2 = 1 - \frac{4\pi R^2}{3A}$ and $K^2 = \left(\sigma_\mu^2 + \sigma_\alpha^2\right)/\left(1 - \frac{4\pi R^2}{3A}\right) + \left(\frac{4\pi R}{A}\right)^2 \sigma_\varepsilon^2/\left(1 - \frac{4\pi R^2}{3A}\right)$. The expression defines a sigmoidal curve , with the radius variability having an important effect (Fig. S3A). The reasons for these dependencies are as follows. For surface-area based size control, both birth and division lengths strongly depend on the true value of the radius and on its variability from cell to cell, as cells with a bigger (smaller) radius divide shorter (longer) and give birth to shorter (longer) daughter cells, like in adder control. A consequence of this correlation is a positive division-birth slope (Fig. 3A), with a theoretical slope given by Eq. (2). This effect was already visible in Fig. 1A: due to area sensing, wider mutants have shorter birth and division lengths (large circles at the bottom-left of the plot), whereas thinner mutant have longer birth and division lengths (small circles at the top-right of the plot). On the contrary, when all the cells have the same radius (i.e. $\sigma_\rho = 0$), the true division length will be perturbed by the sensing error only, and will thus be independent from the length at birth, giving a zero division-birth slope.

To verify whether radius variation can explain the observed division-birth slope based on length, we exploited the natural variability of the radius that is present in wild-type cells. We modulated the variability of the radii of a population of wild-type cells by selecting subsets with a measured radius R^* in the range $R \pm w$. For a given w, we extracted the division-birth slope and radius natural variability of the selected cells (Fig. S3B and Materials and Methods). By gradually reducing w (i.e. by reducing the radius variability), the experimental division-birth slope decreased towards zero as predicted by the model, without any further parameter adjustment (Fig. 3B). We also analysed different combinations of wild-type, thin (*rga2*Δ) and fat (*rga4*Δ) cells. Each combination had a different variability of the radius and, according to our analysis, therefore also a different division-birth slope for length. Model predictions, again without any further parameter adjustment, were in good agreement with the experimental data (Fig. 3C). Overall, these results again support a *pure* area-based sizer control in fission yeast, where variations in the radius cause division-birth slopes based on length to deviate far from zero.

Wild-type data alone supports area-based size control

So far, our analysis has assumed surface area sensing. The previous experiments underpinning this result were based on variability of the cell radius introduced by thin (*rga2*Δ) and fat (*rga4*Δ) mutants [5, 6]. We attempted to overcome this limitation by again exploiting the natural variability of the radius in wild-type cells to verify that area sensing was preserved and was not an artefact due to use of the two mutants.

Following the same procedure used for area sensing, we developed a model based on a length sensing assumption and a model based on a volume sensing assumption (Materials and Methods). For each of the two models, we derived expressions for the CVs at division and the division-birth slopes for the various geometric quantities (length, area, volume). As for area sensing (Fig. 2B), the CV equations were used to estimate the parameters σ_ε , σ_μ and σ_ρ: by tuning their values (separately for length and volume), we found the best fit for the experimental division size CVs for wild-type cells (Fig. 3D). With the obtained parameter values (Table S1), the equations for the division-birth slopes were then used to calculate the theoretical value of the slopes. We found that the experimental CVs but not the experimental wild-type slopes can be reproduced by the model based on a volume sensing assumption, whereas the model based on a length sensing assumption was unable to reproduce either (Figs. 3D-E). On the other hand, the model based on area sensing provided a good fit to both.

Furthermore, for area-based size sensing, one would naively expect that the CV of area at division (A_d^*) should be smaller than that for length (L_d^*), i.e. $\mathrm{CV}^2_{A_d^*} < \mathrm{CV}^2_{L_d^*}$. Our data in Fig. 2B shows that this is only true for sufficiently small experimental measurement errors, σ_ε. This is again expected, since errors in measurement affect the area calculation more than for length, as radius only enters the area estimation. Only when σ_ε is sufficiently small ($\sigma_\varepsilon < R\sigma_\rho$, as predicted by the model, see Materials and Methods) does area sensing emerge as being less variable.

These results indicate both the importance of precise measurements in order to correctly infer the basis of cell size control and, without reliance on mutants, that fission yeast sizer control is indeed based on surface area.

Asymmetric division and defective size sensing can paradoxically appear to enhance sizer behaviour

Besides experimental error and radius variability, the model also includes two further biological sources of variability: asymmetry and sensing precision. We next studied their role in size homeostasis behaviour, based on length measurements.

We showed above how variability in the radius can mask sizer behaviour, bringing the division-birth slope based on length far from zero (Fig. 3B-C). However, for a given value of the radius variability σ_ρ, Eq. 2 indicates that the slope decreases when the asymmetry (σ_α) or the sensing (σ_μ) error increases. This result means that increased errors in the division process (in term of septum positioning and/or size sensing) paradoxically generate better sizing behaviour in a division-birth plot, with a slope closer to zero (Fig. S3A).

These counter-intuitive behaviours can be rationalised as follows: in the case of a perfect sizer, an increase in the asymmetry error does not affect the distribution of the division length. As a consequence, the cloud of points of the division-birth size homeostasis plot is stretched along the x-direction only, causing a reduction of the slope (Fig. 4A). A bigger sensing error produces a wider distribution of both division and birth lengths, i.e. a stretch along both x- and y-directions. However, since the slope value is affected by (reduced) only by the horizontal stretch due to a wider distribution of birth lengths (Materials and Methods), this case turns out to be similar to the asymmetry case. In both cases, the wider spread of the data points reduces the statistical confidence of the slope value. Therefore, to attain similar levels of precision for the slope values as before, a higher number of segmented cells are required (Fig. S4A).

To verify these counter-intuitive predictions about the asymmetry (σ_α) or the sensing (σ_μ) error, we re-examined the case of the *pom1*Δ mutant cells, which divide shorter and often display asymmetric divisions as compared to wild-type cells ($\mathrm{CV}_{L_b^*}$=22% vs 8.4% for the wild-type) [20, 21]. Although formally we cannot exclude that the *pom1* deletion might induce different geometric size sensing, we assume here that *pom1*Δ cells still use surface area for triggering mitosis. Moreover, because of the incompressibility of the G2 phase, cells that have a length at birth above 7-8 µm follow an adder/timer mechanism rather than a sizer mechanism [7] (grey colour in Fig. 4B). Therefore, to avoid interference from this altered size control and to exclude the effects of highly asymmetric divisions, we limited our analysis to cells that start the cell cycle at lengths below ~7 µm (green colour in Fig. 4B). For this subset, the CV of the division length is 9.0%, significantly higher than the wild-type (7.2%), indicating a higher sensing error by this mutant (estimated at $\sigma_\mu \approx 8.6\%$). In agreement with the value of 0.14 predicted by the model, the experimental division-birth slope decreases from +0.25 to +0.15±0.03 (Fig. 4B), making the mutant erroneously appear as a better sizer. For a repeat experiment on agar (Fig. S4B), with a division length CV of 12.2%, the model predicts a slope of 0.08 in good agreement with the experimental measurement of 0.09±0.07.

Model predictions match length- and volume-based sizer control experiments

In a previous work we manipulated fission yeast size sensing in order to generate Cdr2-dependent cell size sensing according to cell length, using the *cdr2-T166A rga2*Δ background. Following this reprogramming, cell division indeed occurred based on length rather than surface area [6]. According to our model for length-based size control, the division-birth slope for length should be zero regardless of the natural variability of the radius and of the segmentation error (Materials and Methods). The experimental value for *cdr2-T166A rga2*Δ of +0.03±0.05 confirms our model prediction and provides additional support for length sensing in this mutant (Fig. 4C).

251 In the same work, we showed that division in the *cdr2*Δ mutant is no longer controlled by area and is instead
252 based on a secondary Cdr2-independent mechanism that moves towards volume control [6]. Similar to
253 *pom1*Δ, data from this mutant can be split into two regimes: a sizer-like regime at shorter cell birth lengths
254 (less than 10 µm) and an adder/timer-like regime for longer cell birth lengths. The division-birth slope
255 obtained for the former regime is 0.47 ±0.04 (Fig. 4D), which, although still (just) closer to sizer than adder
256 behaviour, is even further away from the ideal sizer behaviour than the wild-type. Although the CV of the
257 division length (7.0%) is similar to the wild-type value, an important question to answer is whether *cdr2*Δ is
258 still implementing a sizer.
259
260 For a model based on pure volume sensing, we can again derive the equation for the division-birth slope
261 (Materials and Methods). The equation and the result indicate that the effect of natural variability of the
262 radius is bigger for volume sensing than for area sensing (Fig. 3F). Intuitively, this result follows because cell
263 volume has a quadratic dependence on the radius, whereas area has a linear dependence only. For this
264 reason, the shift of the division-birth slope away from zero will be more pronounced. Without any parameter
265 changing, the model prediction is a slope of +0.62, close to the observed value of around +0.5. Therefore, for
266 *cdr2*Δ, as for all the cases analysed in this study (Fig. 4E), the appearance of more adder-like behaviour is likely
267 due to the use of an incorrect geometrical feature (length) and to the effect of variability in the cell radius.
268
269 **Incorporating a varying radius into the mathematical model**
270 So far, the model was based on the assumption that cell radius does not change from birth to division.
271 Experimental data, however, show a strong, but not perfect, positive correlation between the two
272 measurements ($q = 0.72$, Fig. S5A), indicating that some adjustments in the cell width might occur during the
273 cell cycle. As an additional test, we therefore relaxed the constant radius assumption and developed a
274 generalised mathematical model varying radius from $R_b = R(1+\rho)$ at birth to $R_d = q \cdot R_b + R(1-q)$ at
275 division. These dynamics guarantee the preservation through generations of cell radius around the average
276 value *R*. Numerical simulations show that the key features of the model outcomes are preserved. Moreover,
277 since the variation of radius within one cell cycle is relatively small (Fig. S5A), we did not find significant
278 changes in our results. As a result, the agreement with the experimental evidence is still good (Fig. S5B).
279
280 **Adder behaviour can emerge from pure sizer control**
281 With the exception of length sensing in the *cdr2-T166A rga2*Δ mutant, utilising length as the experimental size
282 measure partially masks pure sizer behaviour by moving the division-birth slope towards adder behaviour, i.e.
283 towards a value of +1. We therefore asked whether the same effect is present in a pure adder mechanism. In
284 particular, we focus on an adder mechanism based on cell volume. This assumption allowed us to develop a
285 model (Materials and Methods) for the widely studied bacterium *E. coli* which shares the same rod-shape as

286 fission yeast and which is believed to utilize cell volume as the key geometrical quantity for size control [22].
287 In contrast with other models [23], also in this adder model we did not include any direct errors on the time
288 durations: rather, variation in the duration of the cell cycle is a consequence of the error in sensing the added
289 size, which is the fundamental quantity monitored by a cell which implements adder control. Similar to our
290 observations for pure sizer control based on volume sensing, the effect of natural cell radius variability causes
291 a monotonic increase of the division-birth length slope from the theoretical adder value of +1 up to +2 (Fig.
292 S6A). By using 3.5% as an estimation of the radius variability [9], our adder model generates a division-birth
293 length slope of +1.51±0.03 (Fig. 5A). Robustness of the outcome was tested by additively
294 increasing/decreasing each standard deviation by up to 1% (or 2%): slope values remained entirely above +1
295 (Fig. S6B). However, all the experimentally reported division-birth length slopes for *E. coli* range from +0.7 to
296 +1 [8, 9], i.e. they never overshoot the theoretical pure adder value. This result may suggest that an adder
297 mechanism is incompatible with the observed behaviour.
298
299 Our results on the *cdr2*Δ mutant revealed that, in the case of a volume-based pure sizer, the effect of radius
300 variability is more pronounced than in the case of area sensing and moves the division-birth length slope
301 much closer to adder-like behaviour. Running a numerical simulation of such a volume-based sizer model with
302 $\sigma_\rho = 3.5\%$ (slightly higher than the radius variability in fission yeast) on *E. coli* sized cells [9], we obtained a
303 division-birth length slope of +0.81±0.02 (Fig. 5B), in agreement with the experimental results from this
304 bacterium. This finding strongly suggests that sizer behaviour in *E. coli* cannot currently be ruled out.
305
306 **DISCUSSION**
307 Phenomenological characterization of size homeostasis is a common approach for extracting information
308 about cell size regulation. Although initial results previously suggested an imperfect or possibly mixed sizer-
309 like control in fission yeast, we have shown here that *pure* sizer control based on *accurate* sensing of cell size
310 is implemented in this organism, using a Cdr2-dependent mechanism with area-based control in the wild-type
311 and length-based control in *cdr2-T166A rga2*Δ [6]. Moreover, we have identified three generalizable aspects
312 in the analyses of size homeostasis: (i) high accuracy in the measurement of the cell size is necessary to avoid
313 misleading data (Fig. 2B); (ii) use of the wrong geometrical quantity (e.g., length instead of area), combined
314 with natural variability of the cell radius, distorts the observed size control behaviours (Fig. 3B-C). While this
315 effect disappears in the presence of length-based sizer sensing (see *cdr2-T166A rga2*Δ, Fig. 4C), the behaviour
316 is even more markedly perturbed when sizer control is based on cell volume (see *cdr2*Δ in Fig. 4D and *E. coli* in
317 Fig. 5B); (iii) asymmetric cell division and, more surprisingly, a reduction in the precision of size sensing, can
318 paradoxically appear to enhance sizer behaviour. As shown by the case of *pom1*Δ in fission yeast, an
319 apparently stronger sizer behaviour (lower division-birth slope) may be due to a loss of precision in size
320 control (Fig. 4B). These demonstrations show that correct interpretation of size homeostasis behaviour

requires accurate measurements of multiple geometrical quantities. Furthermore, “intermediate” behaviour (as in wild-type cells) may not necessarily be due to imperfect size control, nor to a combination of two or more distinct size controls (e.g. sizer and adder). Even limited variability can move the division-birth length slope from 0 towards +1 in the case of pure sizer control and from +1 towards +2 in case of pure adder control, thus completely obscuring the underlying fundamental basis of size control (Fig. 6).

An important aspect that has emerged in our analysis is the effect of radius variability. One might expect that the small variations found from cell to cell might have only a marginal effect on size control behaviour. Surprisingly, the curve and data in Fig. 3C show that, in the case of area-based sizer sensing in fission yeast, a radius variability of only 7% is sufficient to move the division-birth slope close to +1, making pure sizer control wrongly appear as a pure adder. The equations of the model allow us to understand how any particular size homeostasis behaviour can emerge from antagonism between inaccuracy in the division process (asymmetry and size sensing) and radius variability. In the approximation of the slope expression given in Eq. (2), the first non-zero term is $2\sigma_\rho^2/K^2$. If we ignore the contribution of the experimental error σ_ε^2, this term can be approximated by $2\sigma_\rho^2/(\sigma_\alpha^2+\sigma_\mu^2)$, which clearly displays the antagonism between the two effects. In our case, the combination of the estimated values for asymmetry ($\sigma_\alpha = 3.2\%$) and size sensing ($\sigma_\mu = 6.5\%$) errors gives a total standard deviation of 7.3%. Therefore, we can expect that a radius variability of the same order of magnitude can neutralize the effect of these two sources of variation and lead to adder-like behaviour.

For the same reason, despite the adder phenotype, sizer control may still not be ruled out in *E. coli* (Fig. 5), consistent with some alternative theories [12, 22, 24]. Furthermore, according to our analysis, adder control would tend to show behaviour closer to a timer (slope significantly above +1). One caveat is that our adder model considers the simple case of a constant cell size increment from birth to division. It has been alternatively suggested that a constant volume (per origin) is added between two initiations and that cells then divide a constant time after initiation [22]. Although further investigation is needed to better understand this misalignment between the basis of size control and the resulting division-birth slope behaviour, our results suggests that *E. coli* might not implement adder control.

Overall, the analysis presented here shows that pure sizer control is able to reproduce a large variety of cell size homoeostasis behaviours. Our results, with careful attention to both sources of variation in size control and to geometrical aspects preserved by the cell, could be widely relevant in deciphering size homeostasis behaviour in many cell types. Such accurate analyses of cell size behaviours will be critical for dissecting the underlying molecular mechanisms responsible.

355
356 **FIGURES AND TABLES**
357

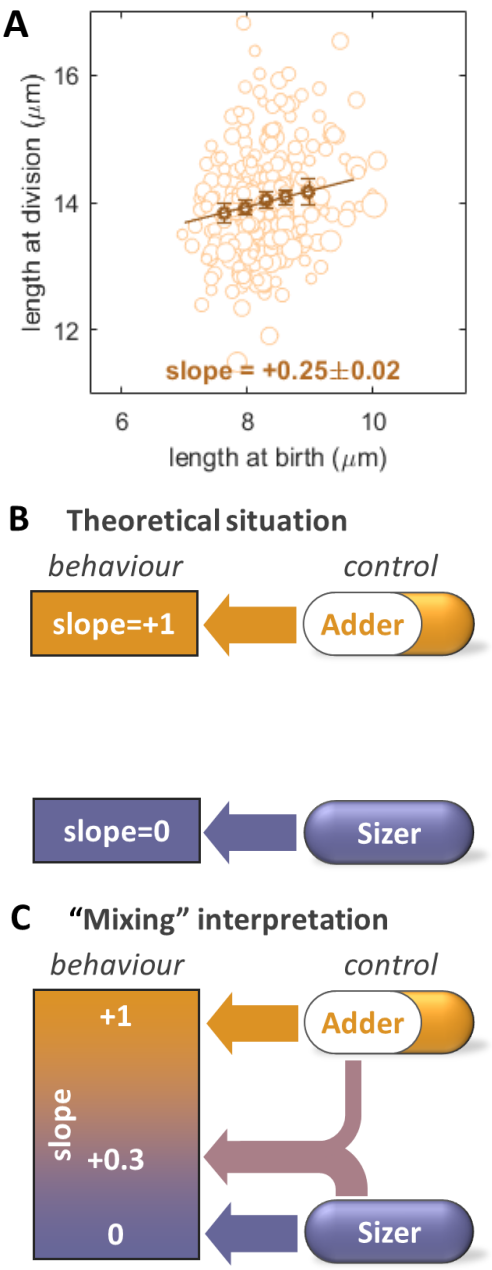

358
359
360
361
362 **Figure 1: Mapping between cell behaviour and underlying basis of size control.** (**A**) Division-birth correlation
363 for wild-type (FC15, n=326) based on measurement of cell length. Size of circles proportional to cell radius.
364 Binned data, with mean value ± standard error, also shown (dark circles), together with best fit line, with
365 indicated slope. (**B**) Theoretical assumption of a one-to-one mapping between division-birth slope and size
366 control, where slope=0 implies sizer control and slope=+1 implies adder control. No intermediate values for
367 the slope are expected. (**C**) Slope values between 0 and +1 could be interpreted as a mix between sizer and
368 adder control (or an imprecise sizer or imprecise adder).
369

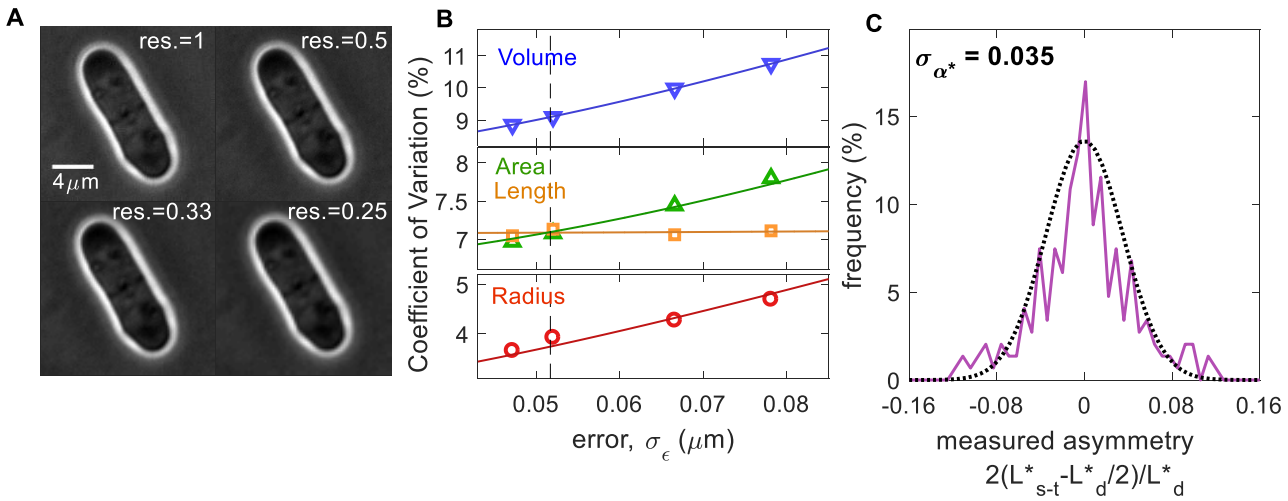

Figure 2: Motivation and model parameter estimation. (**A**) Reduction of image resolution by pixel binning: reported value of resolution is res=1/n, (where n x n pixels have been averaged and condensed into a single pixel; res=1 is the experimentally acquired image). (**B**) Fitting of the observed Coefficient of Variations at division (symbols) by tuning the parameters of the model (curves), at different image resolutions and therefore different experimental errors, σ_ε (wild-type strain FC15, n=326). See also Fig. S1. Dashed line is located where $\sigma_\varepsilon = R\sigma_\rho$: for smaller errors, area sensing becomes apparent, i.e. $\mathrm{CV}^2_{A^*_d} < \mathrm{CV}^2_{L^*_d}$. (**C**) Measurement of division asymmetry and its fitting with a Gaussian distribution to determine σ_α (n=106), where $L^*_{s\text{-}t}$ is the measured distance between the division septum and cell tip. Experimental data are fitted with $\sigma_{\alpha*} = 0.035$. Since $\sigma^2_{\alpha*} \approx \sigma^2_\alpha + 5\sigma^2_\varepsilon/L^2$, we can extract $\sigma_\alpha = 0.032$ (Materials and Methods).

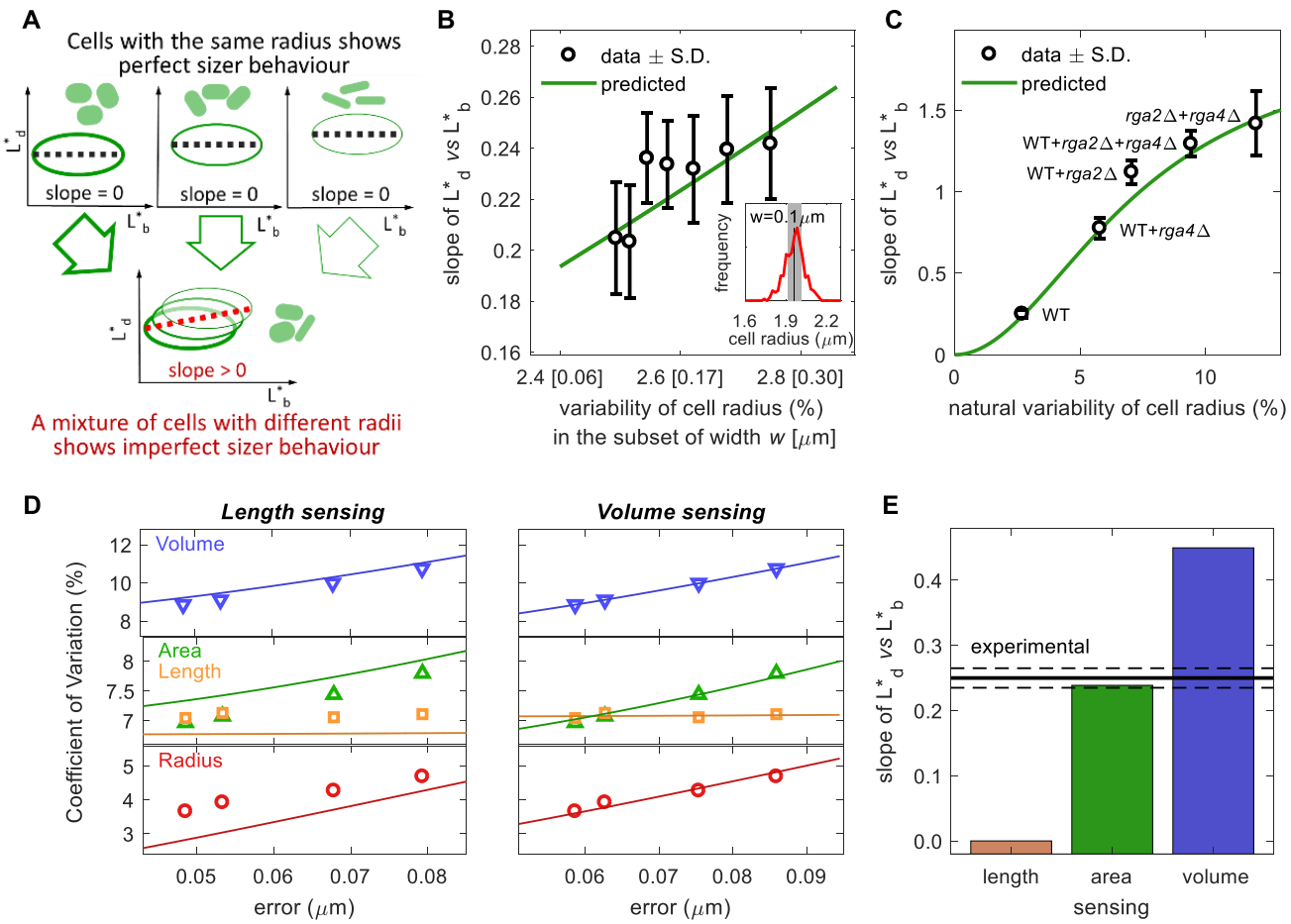

Figure 3: Fission yeast implements a pure area-based sizer (**A**) Intuitive explanation for how, for area sensing, variability in cell radius causes deviation from perfect sizer behaviour. Ellipses represent cloud of data points and dashed lines their linear fitting. (**B**) Inset: radius distribution in red and example of selection of cells with radius in range of ± w = ± 0.1 µm around the mean value (grey shadow). Main plot: for given w (value in squared brackets on x-axis), division-birth slope for length is measured on subset of selected cells (black circle, slope ± SD) and radius variability is calculated (Materials and Methods and Fig. S3B). Predicted slope based on area sensing is calculated with Eq. 2 (green curve). (**C**) Predicted area-based (green curve) and measured division-birth slope for length (mean value ± SD) obtained by combining mutants with different radii. (**D**) Fitting of the observed CV at division (symbols) by tuning the parameters of the model (curves), at different image resolutions and therefore different experimental errors, σ_ε. Left panels: length sensing model. Right panel: volume sensing model (see also Table S1). (**E**) Bars report the theoretical values of division-birth slope for length for each possible geometric size sensing model (based on length, area or volume). Area sensing is the one that provides the best agreement with the experimental data (black line ± SD, continuous and dashed lines). Panel D uses the same data as in Fig. 1A-C. For all other panels data for wildtype strain on agar (FC15, n=326) with automated segmentation.

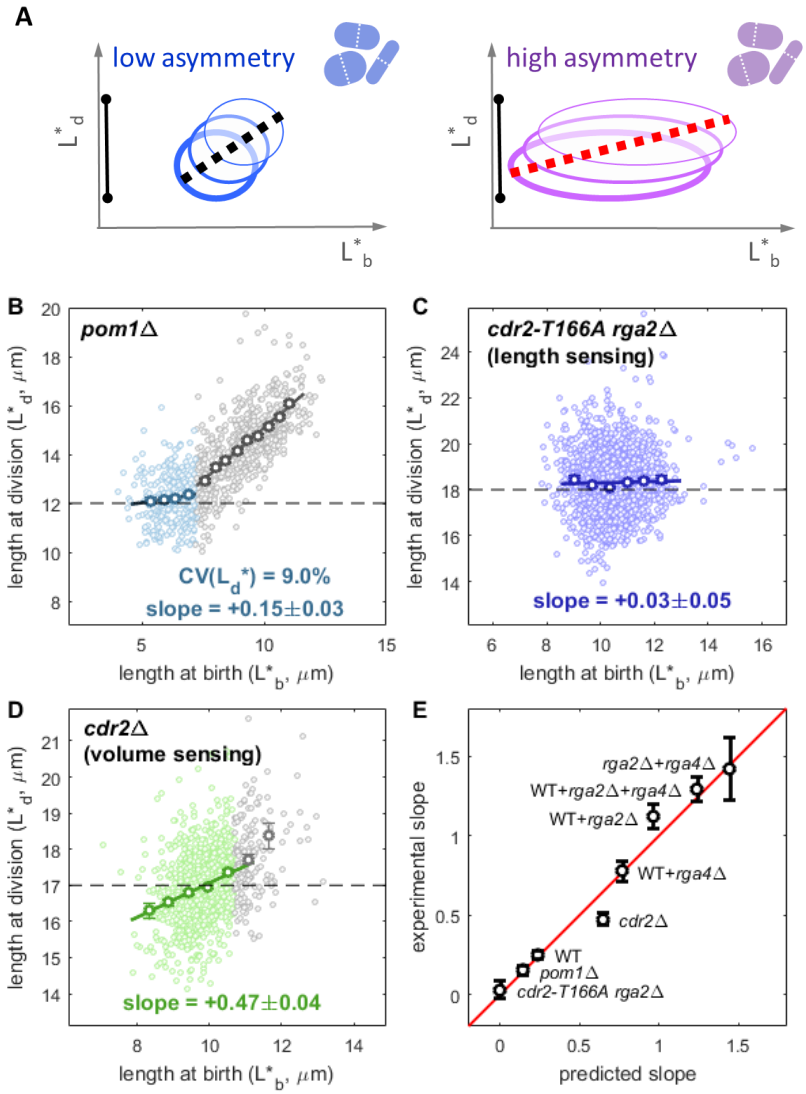

Figure 4: Counter-intuitive predictions arising from asymmetric division errors and consequences of length or volume sensing. (**A**) Possible explanation of how an increase in the asymmetry error at division brings the birth-division slope closer to zero. Black bars indicate the width of the distribution of the division length. (**B**) Size homeostasis plot for *pom1*Δ (FC2063, n=1757, data from [6]). Slopes of reported fit lines are 0.15±0.03 for the sizer regime (green colour, length at birth less than 7 µm) and +0.86±0.03 for the adder/timer-like regime (grey colour, length at birth greater than 7 µm). In the sizer regime, division length has a CV of 9.0%, higher than the wild-type, but has a lower birth-division slope (+0.15 versus +0.25 for the wild-type as reported in Fig. 1A), as predicted by the model. (**C**) Size homeostasis data for the *cdr2-T166A rga2*Δ mutant which implements length sensing shows near perfect sizer behaviour (FC3218, n=1785, data from [6]). (**D**) Size homeostasis data for the *cdr2*Δ mutant, which implements volume sensing. Regression line and reported slope of 0.47±0.04 refers to the binned data with length at birth smaller than 10 µm (green colour). Cells with length at birth greater than 10 µm (grey colour) show a slope of +0.88 ± 0.16 (FC3161, n=1046). Binned data (with mean value ± standard error) shown as bold circles in panels B-D. (**E**) Summary of the agreement between experimental slopes and values obtained by the model. Data points show the mean value ± standard error (see also Fig. S5B).

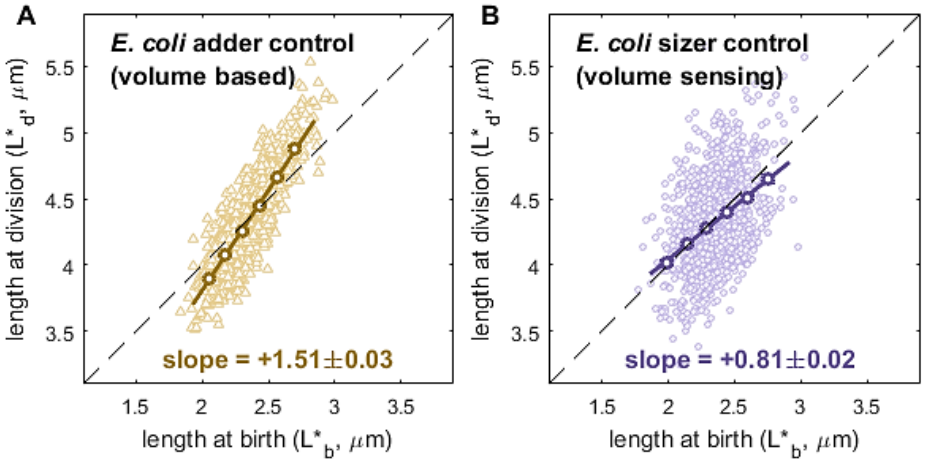

Figure 5: Radius variability and sizer control reproduce the apparent adder behaviour in *E. coli*. (**A**) Simulation of division-birth correlation based on length measurements for *E. coli* utilising pure adder control based on cell volume. (**B**) Same plot in case of pure sizer control based on cell volume. Both plots of panels A and B have been obtained with R=0.55 µm, V=3.77 µm^3, 3.5% as the natural radius variability and the same noise used for fission yeast (Fig. S6B shows the effect of perturbations of these values). Binned data, with mean value ± standard error, also shown (dark circles), as well as best fit line, with indicated slope.

Figure 6: Summary. How a pure sizer mechanism can show a wide range of behaviours. Noise and error lead to an increase of the slope for sizer control (and also for adder control).

TABLE 1: Variables and parameter values of the model.

Symbols	Description	units	Value for each strain				
			WT	*pom1Δ* (subset of short cells only)	*cdr2-T166A rga2Δ*	*cdr2Δ*	*E. coli*
ρ, σ_ρ	Gaussian random variable with standard deviation σ_ρ (value reported here) describing cell-to-cell radius variability	%	2.7	2.7	2.7	2.7	3.5
μ_b, μ_d, σ_μ	Gaussian random variables with standard deviation σ_μ (value reported here) describing cell error in sensing its size	%	6.5	8.6	6.5	6.5	6.5 [a]
α, σ_α	Gaussian random variable with standard deviation σ_α (value reported here) describing the asymmetry in division, defined as $(2L^*_{s-t} - L^*_d)/L^*_d$ where L^*_{s-t} is measured distance between the division septum and cell tip.	%	3.2	3.2	3.2	3.2	3.2 [a]
$\varepsilon_b, \varepsilon_d, \sigma_\varepsilon$	Gaussian random variables with standard deviation σ_ε (value reported here) describing experimental error in the measurement at different resolutions res.=1 (0.0635 µm/pixel) res.=0.5 (0.127 µm/pixel) res.=0.33 (0.190 µm/pixel) res.=0.25 (0.254 µm/pixel)	µm	0.045 0.052 0.067 0.078	0.06 [b]	0.06 [b]	0.06 [b]	0.04 [b]
R	Mean cell radius	µm	1.96	1.89	1.58	1.95	0.55
L	Target cell length at division in case of length sensing (mean of the experimental measurement)	µm	n.a.	n.a.	18.3	n.a.	n.a.
A	Target cell area at division in case of area sensing (mean of the experimental measurement)	μm^2	164	158	n.a.	n.a.	n.a.
V	Target cell volume at division in case of volume sensing (mean of the experimental measurement)	μm^3	n.a.	n.a.	n.a.	183	3.77
q	Persistence of the cell radius from birth to division	-	0.72	0.72	0.72	0.72	-

[a]: Simulations with additively increasing/decreasing each standard deviation by up to 1% (or 2%) are reported in Fig. S6.

[b]: Estimation based on the resolution of the images.

450 **REFERENCES**

451 1. Jun, S., and Taheri-Araghi, S. (2015). Cell-size maintenance: universal strategy revealed. Trends in
452 microbiology *23*, 4-6.
453 2. Chandler-Brown, D., Schmoller, K.M., Winetraub, Y., and Skotheim, J.M. (2017). The adder
454 phenomenon emerges from independent control of pre-and post-start phases of the budding yeast
455 cell cycle. Current Biology *27*, 2774-2783. e2773.
456 3. Sauls, J.T., Li, D., and Jun, S. (2016). Adder and a coarse-grained approach to cell size homeostasis in
457 bacteria. Current opinion in cell biology *38*, 38-44.
458 4. Facchetti, G., Chang, F., and Howard, M. (2017). Controlling cell size through sizer mechanisms.
459 Current Opinion in Systems Biology *5*, 86-92.
460 5. Pan, K.Z., Saunders, T.E., Flor-Parra, I., Howard, M., and Chang, F. (2014). Cortical regulation of cell
461 size by a sizer cdr2p. Elife *3*, e02040.
462 6. Facchetti, G., Knapp, B., Flor-Parra, I., Chang, F., and Howard, M. (2019). Reprogramming Cdr2-
463 Dependent Geometry-Based Cell Size Control in Fission Yeast. Current Biology.
464 7. Wood, E., and Nurse, P. (2013). Pom1 and cell size homeostasis in fission yeast. Cell cycle *12*, 3417-
465 3425.
466 8. Campos, M., Surovtsev, I.V., Kato, S., Paintdakhi, A., Beltran, B., Ebmeier, S.E., and Jacobs-Wagner, C.
467 (2014). A constant size extension drives bacterial cell size homeostasis. Cell *159*, 1433-1446.
468 9. Taheri-Araghi, S., Bradde, S., Sauls, J.T., Hill, N.S., Levin, P.A., Paulsson, J., Vergassola, M., and Jun, S.
469 (2015). Cell-size control and homeostasis in bacteria. Current Biology *25*, 385-391.
470 10. Lin, J., and Amir, A. (2017). The effects of stochasticity at the single-cell level and cell size control on
471 the population growth. Cell systems *5*, 358-367. e354.
472 11. Barber, F., Ho, P.-Y., Murray, A.W., and Amir, A. (2017). Details matter: noise and model structure set
473 the relationship between cell size and cell cycle timing. Frontiers in cell and developmental biology *5*,
474 92.
475 12. Wallden, M., Fange, D., Lundius, E.G., Baltekin, Ö., and Elf, J. (2016). The synchronization of replication
476 and division cycles in individual E. coli cells. Cell *166*, 729-739.
477 13. Soifer, I., Robert, L., and Amir, A. (2016). Single-cell analysis of growth in budding yeast and bacteria
478 reveals a common size regulation strategy. Current Biology *26*, 356-361.
479 14. Banerjee, S., Lo, K., Daddysman, M.K., Selewa, A., Kuntz, T., Dinner, A.R., and Scherer, N.F. (2017).
480 Biphasic growth dynamics control cell division in Caulobacter crescentus. Nature microbiology *2*,
481 17116.
482 15. Fantes, P. (1977). Control of cell size and cycle time in Schizosaccharomyces pombe. Journal of cell
483 science *24*, 51-67.
484 16. Villar-Tajadura, M.A., Coll, P.M., Madrid, M., Cansado, J., Santos, B., and Pérez, P. (2008). Rga2 is a
485 Rho2 GAP that regulates morphogenesis and cell integrity in S. pombe. Molecular microbiology *70*,
486 867-881.
487 17. Das, M., Wiley, D.J., Medina, S., Vincent, H.A., Larrea, M., Oriolo, A., and Verde, F. (2007). Regulation
488 of cell diameter, For3p localization, and cell symmetry by fission yeast Rho-GAP Rga4p. Molecular
489 biology of the cell *18*, 2090-2101.
490 18. Patterson, J.O., Rees, P., and Nurse, P. (2019). Noisy Cell-Size-Correlated Expression of Cyclin B Drives
491 Probabilistic Cell-Size Homeostasis in Fission Yeast. Current Biology.
492 19. Saha, S., and Pollard, T.D. (2012). Anillin-related protein Mid1p coordinates the assembly of the
493 cytokinetic contractile ring in fission yeast. Molecular biology of the cell *23*, 3982-3992.
494 20. Padte, N.N., Martin, S.G., Howard, M., and Chang, F. (2006). The cell-end factor pom1p inhibits mid1p
495 in specification of the cell division plane in fission yeast. Current Biology *16*, 2480-2487.
496 21. Huang, Y., Chew, T.G., Ge, W., and Balasubramanian, M.K. (2007). Polarity determinants Tea1p,
497 Tea4p, and Pom1p inhibit division-septum assembly at cell ends in fission yeast. Developmental cell
498 *12*, 987-996.
499 22. Zheng, H., Ho, P.-Y., Jiang, M., Tang, B., Liu, W., Li, D., Yu, X., Kleckner, N.E., Amir, A., and Liu, C.
500 (2016). Interrogating the Escherichia coli cell cycle by cell dimension perturbations. Proceedings of the
501 National Academy of Sciences *113*, 15000-15005.

502 23. Eun, Y.-J., Ho, P.-Y., Kim, M., LaRussa, S., Robert, L., Renner, L.D., Schmid, A., Garner, E., and Amir, A.
503 (2018). Archaeal cells share common size control with bacteria despite noisier growth and division.
504 Nature microbiology *3*, 148.
505 24. Si, F., Li, D., Cox, S.E., Sauls, J.T., Azizi, O., Sou, C., Schwartz, A.B., Erickstad, M.J., Jun, Y., and Li, X.
506 (2017). Invariance of initiation mass and predictability of cell size in Escherichia coli. Current Biology
507 *27*, 1278-1287.

508